Eur. Phys. J. D **16**, 119–122 (2001)

THE EUROPEAN PHYSICAL JOURNAL D

EDP Sciences

High energy collisions of protonated water clusters

S. Tomita[1,a], J.S. Forster[2], P. Hvelplund[1], A.S. Jensen[1], and S.B. Nielsen[1]

[1] Institute of Physics and Astronomy, University of Aarhus, DK-8000 Aarhus C, Denmark
[2] Department of Engineering Physics, McMaster University, Hamilton, Ontario, Canada L8S 4L7

Received 30 November 2000

Abstract. We have measured attenuation cross sections and fragmentation cross sections for protonated water clusters $H(H_2O)_n^+$ ($n = 1$ to 100) colliding with noble gas atoms (He and Xe) at a laboratory energy of 50 keV. In collisions with He, a transparency effect in the attenuation cross section was observed. For the case of fragmentation in collisions with Xe, a strong enhancement of small clusters was observed which we attribute to multifragmentation.

PACS. 36.40.Qv Stability and fragmentation of clusters – 61.46.+w Nanoscale materials: clusters, nanoparticles, nanotubes, and nanocrystals

1 Introduction

Fragmentation of nuclei, molecules and clusters has attracted considerable interest in recent years. A wide range of materials has been studied such as polymers, colloids, droplets and rocks but so far a complete understanding of fragmentation has not been achieved. Since the fragmentation mechanism is rather independent of the actual system under study, it is worthwhile to study the fragmentation process itself. One approach is a statistical one which has been developed to understand nuclear fragmentation [1]. Many collision induced fragmentation experiments have been made using beams of fullerenes. Although the distribution of fragment abundances is difficult to calculate, considerable success has been obtained by Campbell [2] and Vandenbosch [3] using a statistical approach. In the case of multifragmentation experiments have been carried out by Farizon *et al.* [4] in which they accelerated hydrogen clusters to MeV energies and measured the fragmentation on an event-by-event basis. Multifragmentation of highly charged fullerenes has also been made and analyzed in terms of percolation theory [5]. In this work we present measurements of protonated water clusters and compare the experimental results with statistical calculations.

2 Experiments

A schematic drawing of our apparatus is shown in Fig. 1. Protonated water clusters, $H(H_2O)_n^+$, were generated using an electrospray ion source operated in discharge mode [6]. The source was located on a high voltage platform whose potential was held at 50 kV. After acceleration to 50 keV energy the cluster of interest was selected by a sector magnet and directed at a low pressure gas cell containing either He or Xe gas. Fragment ions were analyzed by a hemispherical electrostatic analyzer situated approximately 1 m downstream of the cell. Cross sections were determined by fitting a polynomial to the intensity of precursor and product ions as a function of target gas pressure. The experimental setup is described in greater detail elsewhere [7].

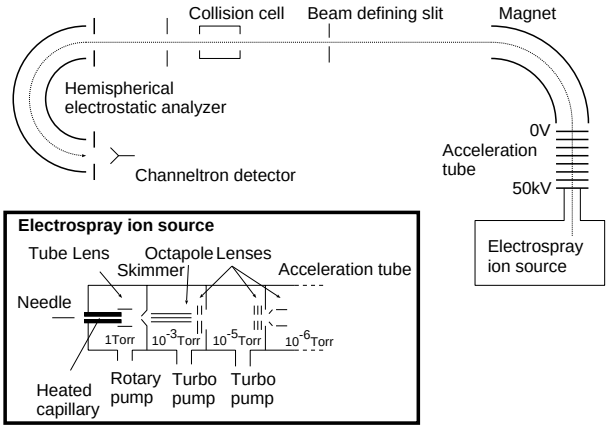

Fig. 1. Schematic drawing of the experimental apparatus.

3 Results and discussion

3.1 Transparency effect

Attenuation cross sections determined by fitting the measured transmitted fractions as a function of target thickness are shown in Fig. 2 for He and Xe. The Xe data show a clear size dependence of $\sigma = \alpha n^{2/3}$ which should

[a] e-mail: tomita@ifa.au.dk

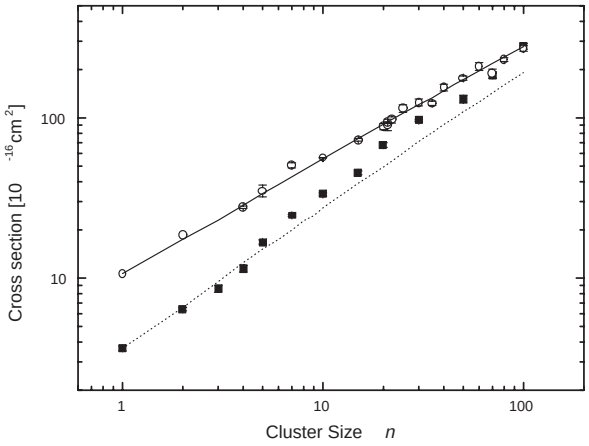

Fig. 2. Attenuation cross sections of protonated water clusters. Open circle and filled square represent measurement with Xe and He respectively. Lines are result of Monte Carlo simulation.

correspond to the geometrical cross section. From a fit to the measured cross sections we obtain a value of $\alpha = 12.4 \times 10^{-16}$ cm^2 in good agreement with the value of 11.4×10^{-16} calculated using the density of water at room temperature. Similar results are obtained for He except for small mass clusters where the cross section is smaller and we believe this to be due to a transparency effect. When the overlap between the water molecule and the He atom is small, the He atom can penetrate the protonated water cluster without causing fragmentation. For small clusters the probability of fragmentation is small because of the overlap between the He and the cluster but for larger clusters the probability of fragmentation increases approaching the geometrical cross section.

To understand this effect we have made Monte Carlo calculations as follows. A random distribution of water molecules within the geometrical structure of a protonated water cluster was made and each water molecule was assumed to have a radius corresponding to that for an individual cross section (*i.e.* the cross section for H_3O^+). Using such random distributions the attenuation cross sections were calculated numerically. The geometrical sizes used in the calculation were taken to be those obtained from the results with the Xe target ($\alpha = 12.4 \times 10^{-16}$ cm^2). Calculations were made for 10 000 initial distributions of the water molecules and the results averaged and plotted as lines in Fig. 2. There is very good agreement between the calculated and measured values. Since the calculations were made with no free parameters, this indicates that the assumption that the energy transfer between the cluster and the target atoms is dominated by elastic collisions in this energy region is reasonable.

3.2 Fragmentation cross sections

A typical fragmentation spectrum is shown in Fig. 3 for $H(H_2O)^+_{70}$ colliding with Xe. Only singly charged fragments are observed with sizes from $m = 4$ to 70. Although $n = 21$ *i.e.* $H(H_2O)^+_{21}$ is known to be magic [8], we have

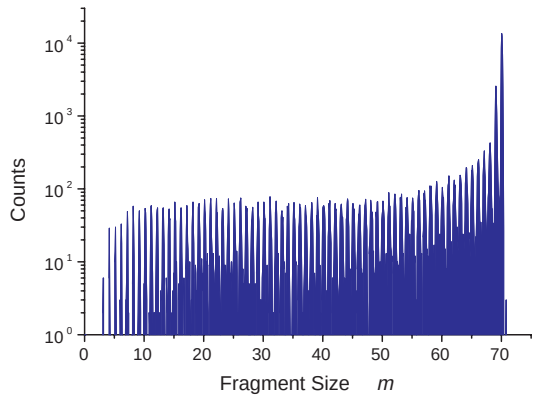

Fig. 3. Fragmentation spectrum of $H(H_2O)^+_{70}$ with Xe target.

observed an enhancement at $n = 21$ only in the mass spectrum from the ion source and in unimolecular rates. No enhancement at $m = 21$ was observed in the fragmentation spectra. Our collision energy is high enough to generate many kinds of isomers, and accordingly this magic number effect might be smeared out. Since no doubly charged clusters are observed, we conclude that the ionization cross section is small compared to the fragmentation cross section.

The 6-nm cross section for producing a fragment $H(H_2O)^+_m$ from the initial $H(H_2O)^+_n$ beam is calculated as follows. The intensity of the precursor cluster after attenuation is given by the total attenuation cross section σ_n^{att} and expressed as

$$I_n = I_0 \exp(-\sigma_n^{att} \rho x) \tag{1}$$

where I_0 is the initial intensity of the precursor cluster beam and ρ and x are the target density and target thickness respectively. The intensity of a fragment ion of cluster size m results not only from direct production from the original beam but also from secondary collisions of larger fragments with the target gas and this can be expressed as

$$I_m = \left(I_{m0} + I_o \sigma_{nm} \rho x + \sum_{n'} \sigma_{nn'} \sigma_{n'm} (\rho x)^2 + \cdots \right) \times \exp(-\sigma_m^{att} \rho x) \tag{2}$$

where I_{m0} represents the intensity of $H(H_2O)^+_m$ due to unimolecular fragmentation of $H(H_2O)^+_n$. Taking the ratio of I_m to I_n and making a series expansion results in

$$\frac{I_m}{I_n} = \frac{I_{m0}}{I_0} + \sigma_{nm} \rho x + \frac{I_{m0}}{I_0} \left(\sigma_n^{att} - \sigma_m^{att} \right) \rho x + \cdots \tag{3}$$

Since, for large m, $\sigma_m^{att} \sim \sigma_n^{att}$ and for small m, unimolecular dissociation is negligible, it is sufficient to include only the first two terms in the expansion. Thus a polynomial fit to I_m/I_n determines the cross section σ_{nm} for $H(H_2O)^+_m$ from $H(H_2O)^+_n$.

Fig. 4 shows fragment production cross sections for beams of $n = 30$, 50 and 70 in He and Xe. We first note that our collision energy is high enough to make small

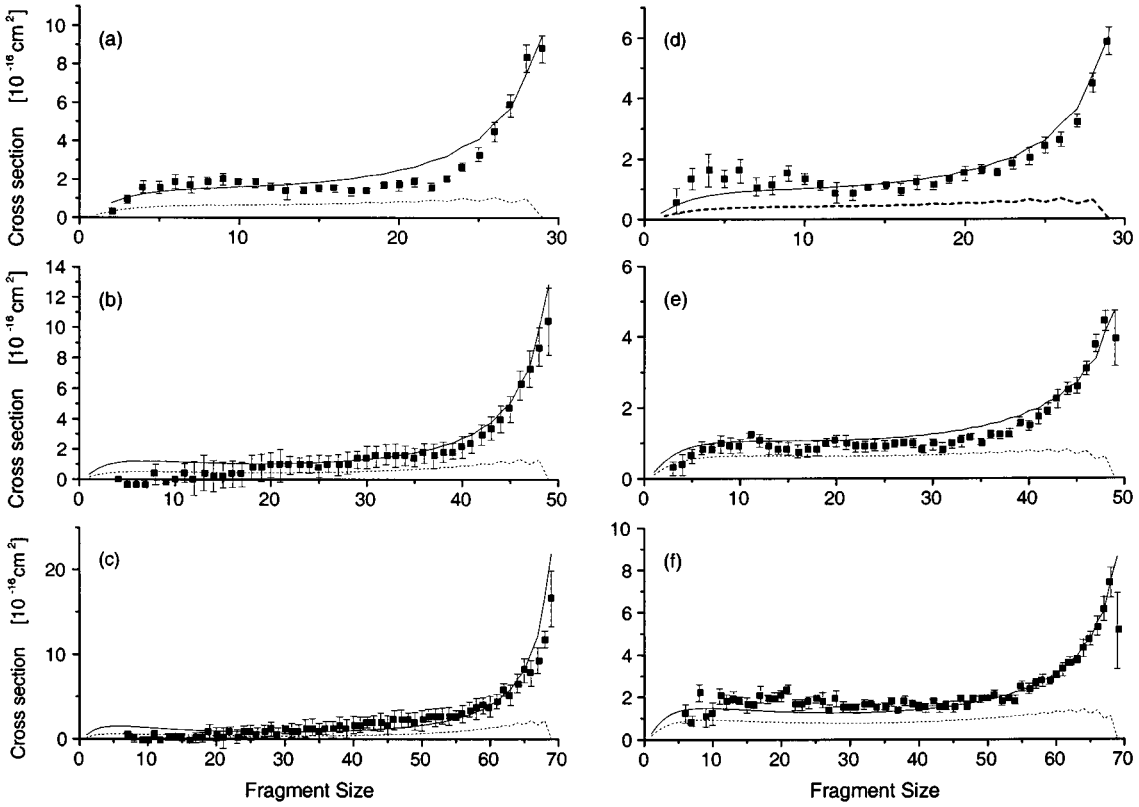

Fig. 4. Fragment production cross section of protonated water cluster $H(H_2O)_n^+$. (a), (b) and (c) are $n = 30$, 50, 70 with He. (d), (e) and (f) are $n = 30$, 50 and 70 with Xe respectively. Lines represent results of statistical calculations, solid lines are the sum of all contributions, dotted lines are contributions of multifragmentation.

clusters. Inspection of Fig. 4 shows a strong similarity in the cross section for production of a given cluster size for the three Xe cases. Further we note the strong similarity between the cases of $n = 30$ in He and Xe in spite of the large difference in CM collision energy. Such target independence has also been observed for hydrogen clusters at very high energy [4]. For the cases of $n = 50$ and $n = 70$ in He there are fewer low mass fragments produced and we attribute this to the low CM collision energy for the heavier beams in He. As described above, the fragmentation process should be violent *i.e.* all fragmentation channels should be open. Therefore, it is convenient to introduce a breakup partition,

$$f\colon \{N_{mq}; 1 \le m \le n, q = 0, 1\} \tag{4}$$

where the number of fragments with cluster size m and charge q is denoted by N_{mq}. For our data the following should be observed

$$\sum_{m,q} N_{mq} m = n, \qquad \sum_{m,q} N_{mq} q = 1 \tag{5}$$

and, for a given partition, the fragment multiplicity is determined by

$$M = \sum_{m,q} N_{mq}. \tag{6}$$

In a statistical treatment, the probability for fragmentation should be proportional to

$$W_f = \frac{1}{\xi} \exp\left(E_f/T\right) \tag{7}$$

$$\xi = \sum_{\text{all partitions}} \exp\left(-E_f/T\right) \tag{8}$$

where E_f and T are the total energy and temperature of the final system. E_f can be written as the sum of translational and binding energies of each fragment

$$E_f = \sum_{m,q} \left[E_k + E_{m,q}\right] N_{mq}. \tag{9}$$

The translational energy is approximated as $T/2$ times the number of translational degrees of freedom, $3M - 3$ (CM motion separated),

$$\sum_{m,q} E_k N_{mq} \simeq \frac{1}{2} \left(3M - 3\right) T. \tag{10}$$

To estimate the binding energy of the fragments we used a liquid drop model assuming a spherical structure with radius r. The binding energy of $H(H_2O)_m$ is expressed as

$$E_n = a_v m - a_s m^{2/3} \tag{11}$$

where a_v and a_s are the coefficients for the volume and surface contributions. For the surface tension we use an experimentally determined expression [9]. When the cluster is protonated, an additional electrostatic term E_c has to be added. The solvation energy is given by [10]

$$E_c = \frac{q^2}{2}\left(1-\frac{1}{\epsilon}\right)\left(\frac{1}{r_i}-\frac{1}{r}\right) \tag{12}$$

where r_i is the radius of the solvated ion, r is the radius of the cluster, ϵ is the permittivity of water and for which an empirical expression is used [11]. To calculate the fragmentation abundances, only the final energy differences are important and we calculated the energy difference of the final states using the initial state Q_f, instead of E_f

$$Q_f = a_s\left(n^{2/3}-\sum_{m,q}N_{mq}m^{2/3}\right)+\frac{1}{2}\left(1-\frac{1}{\epsilon}\right)\frac{1}{r_n} - \sum_{m,q}N_{mq}\frac{q^2}{2}\left(1-\frac{1}{\epsilon}\right)\frac{1}{r_m}\cdot \tag{13}$$

In eq. (13) it is seen that the volume term has disappeared due to the constraint of conservation of total mass and the diameter of the ion inside the water cluster is no longer required since we assume that the ionization cross section is negligible *i.e.* only fragmentation contributes to the final partition. Under this assumption it is possible to include all possible partitions in the calculation. Results of the calculations are shown in Fig. 4 as solid lines. The overall trend of the fragment production cross sections is well reproduced. The results were obtained assuming a temperature of around 645 K which is just below the critical temperature of water. The calculations in Fig. 4 also include the contribution of multifragmentation. As noted above, this contribution is important because of the violence of the collision at the energies used in this work. For $n = 30$ the agreement is somewhat poorer than for the heavier beams. We believe that this is a result of limitations in the liquid drop model since it is not applicable for small sizes as discussed in ref. [8]. Another interesting question is the temperature dependence of the permittivity of the water in a finite system. As seen in eq. (13), surface tension and permittivity are important parameters in the calculations. Since a water molecule has a permanent dipole moment, the permittivity of the water has a strong temperature dependence. This temperature dependence relates to the orientation of the water molecules but in a finite system freedom of orientation would be limited in order to have a bound system. Although we assume the temperature dependence of bulk water we get good agreement between experimental and calculated values indicating that the permittivity of a finite system has a similar value to that of bulk water. Further studies of multifragmentation of these types of cluster should allow us to address this point in more detail.

4 Conclusions

We have measured attenuation cross sections and fragmentation cross sections for protonated water clusters $H(H_2O)_n^+$ ($n = 1$ to 100) colliding with noble gas atoms (He and Xe) at a laboratory energy of 50 keV. For collisions with He a transparency effect in the absorption cross section was observed. The fragmentation cross sections for $H(H_2O)_{50,70}^+$ in He agree with a binary fragmentation process. For the Xe case a strong enhancement is observed in small cluster production. Statistical calculations using a liquid drop approximation reproduce the experimental data well assuming that the water temperature is just below the critical temperature of bulk water. This work represents the first attempt to apply statistical calculations to the fragmentation of clusters in the case of multifragmentation.

This work has been supported by the Danish National Research Foundation through the Aarhus Center for Atomic Physics (ACAP).

References

1. J.P. Bondorf, A.S. Botvina, A.S. Iljinov, I.N. Mishustin, K. Sneppen, Phys. Rep. **257**, 133 (1995).
2. E.E.B. Campbell, T. Raz, R.D. Levine, Chem. Phys. Lett. **253**, 261 (1996).
3. R. Vandenbosch, Phys. Rev. A **59**, 3584 (1999).
4. B. Farizon, M. Farizon, M.J. Gaillard, E. Gerlic, S. Ouaskit, Nucl. Instr. Meth. Phys. Res. B **88**, 86 (1994).
5. S. Cheng, H.G. Berry, R.W. Dunford, H. Esbensen, D.S. Gemmell, E.P. Kanter, T. LeBrun, W. Bauer, Phys. Rev. A **54**, 3182 (1996).
6. S. König, H.M. Fales, J. Am. Soc. Mass Spectrom. **9**, 814 (1998).
7. O.V. Boltalina, P. Hvelplund, T.J.D. Jørgensen, M.C. Larsen, M.O. Larsson, D.A. Sharoitchenko, Phys. Rev. A **62**, 023202 (2000).
8. Z. Shi, V. Ford, A.W. Castleman Jr, J. Chem. Phys. **99**, 8009 (1993).
9. N.B. Vargaftik, B.N. Volkov, L.D. Voljak, J. Phys. Chem. Ref. Data **12**, 817 (1983).
10. B. Roux, H.A. Yu, M.J. Karplus, J. Phys. Chem. **94**, 4683 (1990).
11. D.P. Fernández, A.R.H. Goodwin, E.W. Lemmon, J.M.H. Levelt Sengers, R.C. Williams, J. Phys. Chem. Ref. Data **26**, 1125 (1997).